Are Land-Use Change Emissions in Southeast Asia Decreasing or Increasing?

Masayuki Kondo[1,2] ![ID], Stephen Sitch[3] ![ID], Philippe Ciais[4] ![ID], Frédéric Achard[5], Etsushi Kato[6] ![ID], Julia Pongratz[7,8], Richard A. Houghton[9], Josep G. Canadell[10] ![ID], Prabir K. Patra[11] ![ID], Pierre Friedlingstein[12], Wei Li[13] ![ID], Peter Anthoni[14] ![ID], Almut Arneth[14], Frédéric Chevallier[4] ![ID], Raphael Ganzenmüller[7] ![ID], Anna Harper[12] ![ID], Atul K. Jain[15] ![ID], Charles Koven[16] ![ID], Sebastian Lienert[17], Danica Lombardozzi[18] ![ID], Takashi Maki[19], Julia E. M. S. Nabel[8] ![ID], Takashi Nakamura[20], Yosuke Niwa[2], Philippe Peylin[4], Benjamin Poulter[21] ![ID], Thomas A. M. Pugh[22,23,24] ![ID], Christian Rödenbeck[25], Tazu Saeki[2] ![ID], Benjamin Stocker[26] ![ID], Nicolas Viovy[4], Andy Wiltshire[27] ![ID], and Sönke Zaehle[25] ![ID]

[1]Institute for Space-Earth Environmental Research, Nagoya University, Nagoya, Japan, [2]Center for Global Environmental Research, National Institute for Environmental Studies, Tsukuba, Japan, [3]College of Life and Environmental Sciences, University of Exeter, Exeter, UK, [4]Laboratoire des Sciences du Climat et de l'Environnement, Institut Pierre Simon Laplace, Gif-sur-Yvette, France, [5]Directorate D – Sustainable Resources, Joint Research Centre of the European Commission, Ispra, Italy, [6]Institute of Applied Energy, Tokyo, Japan, [7]Department of Geography, Ludwig-Maximilians-Universität München, Munich, Germany, [8]Land in the Earth System, Max Planck Institute for Meteorology, Hamburg, Germany, [9]Woodwell Climate Research Center, Falmouth, MA, USA, [10]Global Carbon Project, Commonwealth Scientific and Industrial Research Organisation–Oceans and Atmosphere, Canberra, ACT, Australia, [11]Department of Environmental Geochemical Cycle Research, Japan Agency for Marine–Earth Science and Technology, Yokohama, Japan, [12]College of Engineering, Mathematics and Physical Sciences, University of Exeter, Exeter, UK, [13]Ministry of Education Key Laboratory for Earth System Modeling, Department of Earth System Science, Tsinghua University, Beijing, China, [14]Institute of Meteorology and Climate Research/Atmospheric Environmental Research, Karlsruhe Institute of Technology, Garmisch–Partenkirchen, Germany, [15]Department of Atmospheric Sciences, University of Illinois at Urbana–Champaign, Urbana, IL, USA, [16]Earth Sciences Division, Lawrence Berkeley National Laboratory, Berkeley, CA, USA, [17]Climate and Environmental Physics, Physics Institute and Oeschger Centre for Climate Change Research, University of Bern, Bern, Switzerland, [18]Climate and Global Dynamics, National Center for Atmospheric Research, Boulder, CO, USA, [19]Meteorological Research Institute, Tsukuba, Japan, [20]Japan Meteorological Agency, Tokyo, Japan, [21]National Aeronautics and Space Administration Goddard Space Flight Center, Biospheric Science Laboratory, Greenbelt, MD, USA, [22]Department of Physical Geography and Ecosystem Science, Lund University, Lund, Sweden, [23]Department of Geography, Earth and Environmental Science, University of Birmingham, Birmingham, UK, [24]Birmingham Institute of Forest Research, University of Birmingham, Birmingham, UK, [25]Max Planck Institute for Biogeochemistry, Jena, Germany, [26]Department of Environmental Systems Science, ETH Zürich, Zürich, Switzerland, [27]Met Office Hadley Centre, Exeter, UK

Abstract Southeast Asia is a region known for active land-use changes (LUC) over the past 60 years; yet, how trends in net CO_2 uptake and release resulting from LUC activities (net LUC flux) have changed through past decades remains uncertain. The level of uncertainty in net LUC flux from process-based models is so high that it cannot be concluded that newer estimates are necessarily more reliable than older ones. Here, we examined net LUC flux estimates of Southeast Asia for the 1980s−2010s from older and newer sets of Dynamic Global Vegetation Model simulations (TRENDY v2 and v7, respectively), and forcing data used for running those simulations, along with two book-keeping estimates (H&N and BLUE). These estimates yielded two contrasting historical LUC transitions, such that TRENDY v2 and H&N showed a transition from increased emissions from the 1980s to 1990s to declining emissions in the 2000s, while TRENDY v7 and BLUE showed the opposite transition. We found that these contrasting transitions originated in the update of LUC forcing data, which reduced the loss of forest area during the 1990s. Further evaluation of remote sensing studies, atmospheric inversions, and the history of forestry and environmental policies in Southeast Asia supported the occurrence of peak emissions in the 1990s and declining thereafter. However, whether LUC emissions continue to decline in Southeast Asia remains uncertain as key processes in recent years, such as conversion of peat forest to oil-palm plantation, are yet to be represented in the forcing data, suggesting a need for further revision.

1. Introduction

Following a long debate about the contribution of tropical regions (i.e., Amazon basin, tropical Africa, and Southeast Asia) to the global CO_2 budget (Gurney et al., 2002, 2003, 2004; Stephens et al., 2007), recent assessments are converging to the agreement that the regions are nearly carbon-neutral as a whole (Gaubert et al., 2019; Kondo et al., 2020; Schimel et al., 2015; Stephens et al., 2007). Carbon sequestration by photosynthesis is believed to be largest in tropical regions due to a presumably strong effect of CO_2 fertilization (Keenan et al., 2016; Kondo, Ichii, Patra, Poulter, et al., 2018; Schimel et al., 2015), in turn suggesting that a comparably large amount of CO_2 is emitted from those regions. Severe drought caused by El Niño–Southern Oscillation (ENSO) and extensive ecosystem loss and conversion by land-use changes (LUC) are the two major factors of CO_2 emissions in tropical regions (Brando et al., 2019; Clark, 2004; Kondo, Ichii, Patra, Canadell, et al., 2018). As evidenced by previous findings, Southeast Asia is particularly susceptible to those factors, such as high tree mortality rates and fire emissions due to droughts (Brando et al., 2019; Hooijer et al., 2010; Huijnen et al., 2016; Page et al., 2002; Patra, Ishizawa, et al., 2005; Qie et al., 2017; Siegert et al., 2001; Thirumalai et al., 2017) and persistent high deforestation rate (Achard et al., 2004, 2014).

Although both ENSO and LUC are essential factors for CO_2 emissions of Southeast Asia, LUC is of utmost importance because of its long-term influence on CO_2 fluxes. Particularly, deforestation has been active in Southeast Asia from the 1960s to the present (FAO, 2011) and has mainly affected lowlands, but recently expanded to mountainous highlands (Zeng et al., 2018). The integration of remote sensing and inventory data indicates that a net change of aboveground carbon in Southeast Asia is a loss of 28.2 Tg C yr^{-1} for 2003–2014 (Baccini et al., 2017), implying greater CO_2 emissions from LUC activities than the CO_2 uptake in forest regrowth (Kondo, Ichii, Patra, Canadell, et al., 2018; Pugh et al., 2019) and intact old-growth forest (Lewis et al., 2009). To reduce high CO_2 emissions from deforestation in Southeast Asia and other tropical regions, an international effort to Reduce Emissions from Deforestation and forest Degradation (REDD+) was proposed and agreed to by the United Nations Framework Convention on Climate Change (UNFCCC). Yet, in estimating baselines for REDD + activities, the science community is challenged with estimating current regional LUC emissions from multiple unpredictable factors, such as wood and crop harvest, deforestation, degradation, shifting cultivation, and conversion of peat forest to oil-palm plantation (Grassi et al., 2018; Mitchard, 2018), which cannot all be constrained by observations with the required reliability. To date, despite the urgent need from policymakers, high uncertainty remains in our understanding of the historical LUC transition and associated CO_2 emissions in Southeast Asia, which has made it difficult to determine whether the current trend in LUC emissions is decreasing or increasing.

At present, process-based Dynamic Global Vegetation Models (DGVMs) are one of the key carbon accounting tools for estimating CO_2 uptake and release induced by LUC activities (Sitch et al., 2015). Since 2013, an international collaboration under the umbrella of the Global Carbon Project has annually assessed and reported the global state of the CO_2 budget in the land and ocean (Global Carbon Budget [GCB]: Le Quéré et al., 2013, 2014, 2016; Le Quéré, Moriarty, Andrew, Peters, et al., 2015; Le Quéré, Moriarty, Andrew, Canadell, et al., 2015; Le Quéré, Andrew, Friedlingstein, Sitch, Hauck, et al., 2018; Le Quéré, Andrew, Friedlingstein, Sitch, Pongratz, et al., 2018) (Friedlingstein et al., 2019), and of associated component fluxes including net LUC flux estimated by a set of DGVMs assembled under the TRENDY project (Sitch et al., 2015). While most global fluxes reported in a series of the GCB papers (e.g., fossil-fuel emissions, net ocean flux, and natural land vegetation flux) have consistency in interannual variability and trend, the global net LUC flux estimates from DGVMs have undergone a drastic change. Up to the GCB 2014 (i.e., GCB 2013 and 2014), DGVMs estimated the largest global LUC emissions for the period 1960s−2010s in the 1990s (1.8–2.0 Pg C yr^{-1}), whereas starting with the GCB 2015 (i.e., GCB 2015–2018), this peak was largely reduced (1.2–1.3 Pg C yr^{-1}), making the net LUC flux relatively stable through the past decades (Figure S1 in Supporting Information S1). Although this update may affect regional estimates of net LUC flux, especially for regions characterized by active LUC (e.g., tropical regions including Southeast Asia), it has not been dealt with or even acknowledged, leaving causes of the change unknown.

Given the high uncertainty about the net LUC flux estimates, this study attempts to identify a plausible historical LUC transition for Southeast Asia through a comprehensive comparison of DGVM simulations. We examined net LUC flux estimates for the 1980s to 2010s from the two versions of TRENDY used in the GCB 2013 (TRENDY v2, Le Quéré et al., 2014) and 2018 (TRENDY v7, Le Quéré, Andrew, Friedlingstein, Sitch, Hauck, et al., 2018), and LUC forcing data used for running those TRENDY versions, along with two book-keeping estimates of net LUC flux (Hansis et al., 2015; Houghton & Nassikas, 2017). Further, we investigated a pattern of LUC transitions

Table 1
Methodologies of the Net LUC Flux Estimation by 10 DGVMs From TRENDY v2 and v7

Description of land-use and land-cover change modeling method

Method 1	HYDE-based summed transitions (ST_HYD): LUC modeling method using a sum of the HYDE cropland and pasture area. Changes in summed cropland and pasture area correspond to those of simulated ecosystem land area (forests, grasslands, and others) in DGVMs.
Method 2	LUH-based summed transitions (ST_LUH): LUC modeling method using a sum of the LUH primary and secondary land fractions. Changes in primary and secondary land area fractions correspond to those of simulated ecosystem land area (forests, grasslands, and others) in DGVMs.
Method 3	LUH-based distinguished transitions (DT_LUH): LUC modeling method using the LUH land cover types distinguished (e.g., primary and secondary land area distinguished).

Transition of land use and land cover change modeling approach between TRENDY v2 and v7

DGVM	CLM	ISAM	JSBACH	JULES	LPJ-wsl	LPJ-GUESS	LPX-Bern	O-CN	ORCHIDEE	VISIT
TRENDY v2 (GCB2013)	Method2 (ST_LUH1)	Method2 (ST_LUH1)	Method2 (ST_LUH1)	Method1 (ST_HYD31)	Method1 (ST_HYD31)	Method1 (ST_HYD31)	Method2 (ST_LUH1)	Method1 (ST_HYD31)	Method1 (ST_HYD31)	Method3 (DT_LUH1)
TRENDY v7 (GCB2018)	Method2 (ST_LUH2)	Method2 (ST_LUH2)	Method2 (ST_LUH2)	Method1 (ST_HYD32)	Method3 (DT_LUH2)	Method3 (DT_LUH2)	Method2 (ST_LUH2)	Method2 (ST_LUH2)	Method2 (ST_LUH2)	Method3 (DT_LUH2)

Note. ST_HYD31 (summed transitions using HYDE v3.1), ST_HYD32 (summed transitions using HYDE v3.2), ST_LUH1 (summed transitions using LUH v1), ST_LUH2 (summed transitions using LUH v2), DT_LUH1 (distinguished transitions using LUH v1), and DT_LUH2 (distinguished transitions using LUH v2).

through independent evaluations of forest area changes from remote sensing studies, atmospheric inversions to constrain total terrestrial CO_2 fluxes, and the history of forestry and environmental policies. Lastly, we discuss factors and uncertainties in current LUC modeling for Southeast Asia.

2. Methods

2.1. Region

The Southeast Asia region of this study comprises 12 countries including the Association of Southeast Asian Nations (ASEAN) countries (Brunei Darussalam, Cambodia, Indonesia, Lao PDR, Malaysia, Myanmar, Philippines, Singapore, Thailand, Vietnam), and non-ASEAN member countries (East Timor, and Papua New Guinea). Note that it is different from the United Nations geoscheme for Southeast Asia. This regional definition used National Identifier Grid v4.11 (https://sedac.ciesin.columbia.edu/data/set/gpw-v4-national-identifier-grid-rev11/) to identify nations of Southeast Asia. All results presented in this study are based on this definition of Southeast Asia.

2.2. Process-Based Estimate of Net LUC Flux

2.2.1. Dynamic Global Vegetation Models

Process-based estimates of the net LUC flux were represented by simulations of the 10 DGVMs that participated in both TRENDY v2 (used in Le Quéré et al., 2014) and v7 (Le Quéré, Andrew, Friedlingstein, Sitch, Hauck, et al., 2018); they are CLM, ISAM, JSBACH, JULES, LPJ-wsl, LPJ-GUESS, LPX-Bern, O-CN, ORCHIDEE, and VISIT (Table 1). Simulations of the TRENDY models were prepared with a consistent forcing data set (Table S1 in Supporting Information S1): atmospheric CO_2 concentrations based on ice core measurements and stationary observations from the National Oceanic and Atmospheric Administration (NOAA), gridded climate data set (CRU-NCEP for TRENDY v2 and CRU-JRA for TRENDY v7), and gridded annual land-use land-cover change datasets: the HistorY Database of the global Environment (HYDE: Klein Goldewijk et al., 2011, 2017) and Land-Use Harmonization (LUH: Hurtt et al., 2011, 2020). In between these TRENDY versions, several of the models have experienced major updates, including changes towards more sophisticated representations of LUC modeling (see Table 6 in Le Quéré et al., 2014, Table 6 in Le Quéré, Moriarty, Andrew, Canadell, et al., 2015; Le Quéré et al., 2016, and Table 4 in Le Quéré, Andrew, Friedlingstein, Sitch, Pongratz, et al., 2018; Le Quéré, Andrew, Friedlingstein, Sitch, Hauck, et al., 2018). Details and characteristics of the DGVMs are summarized in Le Quéré et al. (2014) for TRENDY v2 and Le Quéré, Andrew, Friedlingstein, Sitch, Hauck, et al. (2018) for v7.

The TRENDY models provided three types of simulations: (a) one that considers the variability in atmospheric CO_2 (S1), (b) one that considers the variability in CO_2 and climate (S2), and (c) one that considers the variability in CO_2, climate, and historical land use and land cover changes (S3). The net CO_2 flux of the S3 simulation represented the most realistic estimate, including attributes of CO_2 fertilization, climate variability, and LUC on the net CO_2 flux. Those from the S1 and S2 simulations represented the partial contributions to net CO_2 flux, signifying the CO_2 fertilization in S1 and CO_2 fertilization and climate variability in S2. The net LUC flux was extracted via isolating the contribution of LUC variability on the net CO_2 flux, specifically by subtracting a net CO_2 flux estimate of the S2 simulation (accounting for CO_2 fertilization and climate variability) from that of the S3 simulation (accounting for CO_2 fertilization, climate, and LUC variability).

2.2.2. LUC Forcing and Modeling

The LUC forcing for the TRENDY models (i.e., HYDE and LUH) provides gridded historical transitions of land-use and land-cover changes, based on annual cropland and pasture area and wood harvest from the U.N. Food and Agricultural Organization (FAO) national statistics. Historical changes in annual area of cropland and pasture were determined by HYDE, which takes the FAO national statistics for cropland (the FAO categories of "arable land" and "cropland") and pasture (the FAO category of "permanent meadow and pastures") as the main input source. HYDE spatializes the FAO statistics using allocation algorithms and time-dependent weighting maps based on global historical population density, soil suitability, distance to rivers, lakes, slopes, and biome distributions. HYDE maintains FAO cropland and pasture total area and relative fraction in each country while spatially distributing the area within national borders. In between TRENDY v2 and v7, HYDE was updated from v3.1 (Klein Goldewijk et al., 2011) to v3.2 (Klein Goldewijk et al., 2017). In the v3.1, cropland and pasture areas were allocated with predefined rules, such as that land with the highest soil suitability for crops is colonized first, coastal areas and river plains are more favorable for early settlement, and no allocation is allowed in urban built-up areas or high population density. In the v3.2, the allocation algorithm was changed from the predefined rules-based methods to more statistical methods (i.e., probability-based allocations) using the high-resolution ESA Land Cover maps from the ESA Climate Change Initiative (ESA, 2017). In addition, in the v3.2, cropland was further categorized into irrigated and rain-fed crops, and pasture (termed grazing land in HYDE v3.2) was categorized into intensively used pasture and less intensively used rangeland. Note that this study evaluates the HYDE v3.1 and v3.2 data prepared for the GCB 2013 and GCB 2018, which may reflect minor changes from the publicly available HYDE data (https://www.pbl.nl/en/image/about-image).

LUH further combined the HYDE cropland and pasture status with the wood harvest status based on the FAO national wood harvest statistics to extend global LUC patterns, including transitions of cropland, pasture, and primary and secondary forest, and primary and secondary non-forest (including grassland and shrub). A sum of primary forest and primary non-forest is referred to as primary land and a sum of secondary forest and secondary non-forest is secondary land, hereafter. First, the original $5' \times 5'$ resolution cropland and pasture areas of HYDE were aggregated to coarser resolutions ($0.5° \times 0.5°$ in the older version and $0.25° \times 0.25°$ in the newer version of LUH), and fractions occupied by those lands were calculated for each rescaled grid cell. By subtracting fractions of cropland and pasture (and water/ice, if any) from each grid cell, fractions of natural vegetation (primary and secondary forest and non-forest) were also determined for each grid cell. Distinction between primary and secondary forest, and primary and secondary non-forest, and fractions of these land types occupied in each grid cell were determined based on the spatialized FAO wood harvest data with empirically estimated biomass density maps produced from Miami-LU model (Hurtt et al., 2011). In between TRENDY v2 and v7, LUH was updated from v1 (Hurtt et al., 2011) to v2 (Hurtt et al., 2020), which includes new features, such as an increase in cropland sub-categories (annual and perennial C3 and C4, etc.), and finer spatial resolutions of grid-cell from 0.5° to 0.25° degrees. Additionally, in the v2, the algorithm for estimating the spatial pattern of forest transitions due to wood harvesting was constrained by a gridded forest loss estimate based on Landsat from Hansen et al., (2013). Also, a base global map for the shifting cultivation algorithm was changed from the pioneer global shifting cultivation map known as Butler map (Butler, 1980), to Heinimann map: an improved Butler map with a few modifications reflecting high-resolution satellite imagery and extensive expert survey (Heinimann et al., 2017). As in HYDE, note that this study evaluates the LUH v1 and v2 data prepared for the GCB 2013 and GCB 2018, which may reflect minor changes from the publicly available LUH data (https://luh.umd.edu/index.shtml).

The choice and use of the LUC forcing data differ among DGVMs (Table 1). The net LUC flux of DGVMs accounts for the net effect of LUC on the terrestrial carbon cycle, including instantaneous and legacy emissions,

and regrowth flux, but specific schemes for LUC modeling were left to the discretion of each modeling group, which means that fundamental assumptions and levels of complexity in LUC modeling vary among the DGVMs. Particularly, major differences in the method of LUC modeling include whether to use HYDE or LUH as forcing data, and the extent to which the information provided by those LUC forcing data are used. The differences are overall as follows. DGVMs that use HYDE as the LUC forcing update simulated forest and non-forest (including grassland and shrub) cover in response to a sum of annual changes in prescribed cropland and pasture area. Thus, in those DGVMs, an increase in cropland and pasture areas corresponds to a decrease in simulated forest and non-forest area, and vice versa. We refer to this method of LUC modeling as method 1: HYDE-based summed (cropland and pasture area) transitions (Table 1). DGVMs that used LUH as the LUC forcing make transitions of simulated forest and non-forest cover in response to annual changes in prescribed primary and secondary land area fractions (here, "land" refers to a sum of forest and non-forest). Thus, in those DGVMs, changes in primary and secondary land areas directly correspond to those in simulated forest and non-forest areas. Yet, this approach differs in using the prescribed information as a sum (primary and secondary land area combined) or separate components (primary and secondary land area distinguished). We refer to the former method as method 2: LUC-based summed transitions and the latter method as method 3: LUC-based distinguished transitions (Table 1). In TRENDY v2 and v7, one out of 10 DGVMs used method 1 (i.e., JULES), four used method 2 (i.e., CLM, ISAM, JSBACH, and LPX-Bern), and one used method 3 (i.e., VISIT). For the other four DGVMs (i.e., LPJ-wsl, LPJ-GUESS, O-CN, and ORCHIDEE), the LUC modeling based on method 1 in TRENDY v2 was changed to method 2 or method 3 in TRENDY v7 (Table 1).

2.3. Book-Keeping Models

In addition to the DGVMs, two book-keeping models, H&N (Houghton & Nassikas, 2017) and BLUE (Hansis et al., 2015), were evaluated. Based on national statistics, the book-keeping method tracks changes in the carbon stored in vegetation and soil due to LUC, such as deforestation, wood harvest, crop cultivation, and shifting cultivation. H&N estimates national-level net LUC flux based directly on the national statistics of five-year changes in forest area and management from the Forest Resources Assessment (FRA) 2015 report (FAO, 2015) and annual changes in cropland and pasture area from FAOSTAT (http://www.fao.org/faostat/en/#data), while BLUE (as used in Le Quéré, Andrew, Friedlingstein, Sitch, Hauck, et al., 2018) estimates spatially explicit net LUC flux using annual changes in primary and secondary forest, cropland, pasture, and rangeland fractions from the LUH v2 (method 3 of the DGVMs' LUC modeling with forest, non-forest, and other ecosystem types treated separately) In addition, BLUE was rerun here using LUH v1 with the same model configurations. In the comparison of this study, we did not add LUC-related fire emissions (e.g., deforestation fire and peat burning) to those book-keeping estimates as this kind of land use is not well represented in most DGVMs. Further details and characteristics of these methods are provided in the original publications and summarized in Le Quéré, Andrew, Friedlingstein, Sitch, Hauck, et al. (2018) and Friedlingstein et al. (2019).

2.4. Atmospheric CO_2 Inversions Constrained by Regional Aircraft CO_2 Observations

Emissions of CO_2 from LUC activities are a major component of the net CO_2 flux in Southeast Asia (Kondo, Ichii, Patra, Canadell, et al., 2018); therefore, the temporal variability in the net CO_2 flux should closely follow that of the net LUC flux. To evaluate LUC transitions in this study, the net CO_2 flux from TRENDY v2 and v7 (S3 simulation) were compared with independent estimates of three inversion systems: ACTM (Saeki & Patra, 2017), JMA2018 (Maki et al., 2010), and NICAM-TM (Niwa et al., 2012). These inversions estimate the net land and ocean CO_2 fluxes by fitting modeled CO_2 concentrations against continuous and discrete atmospheric CO_2 measurements from global networks (e.g., NOAA Earth System Research Laboratory, World Data Centre for Greenhouse Gases, and Comprehensive Observation Network for TRace gases by AIrLiner: CONTRAIL) with prior information (e.g., land and ocean fluxes and fossil fuel emissions). One may question the reliability of atmospheric inversions for Southeast Asian CO_2 flux estimation as there are no in-situ atmospheric CO_2 measurements for that region (only in nearby regions). In this circumstance, aircraft CO_2 measurements (e.g., the CONTRAIL Japan Airlines Narita-Sydney line) are the key data for capturing the signals of CO_2 fluxes over Southeast Asia (Niwa et al., 2012; Patra, Ishizawa, et al., 2005; Patra, Maksyutov, et al., 2005). For this reason, we limited atmospheric inversions to the three that used the aircraft CO_2 measurements over Southeast Asia for assimilation and that fully

covered the 1990s. Further details and characteristics of these models are provided in the corresponding literature and summarized in Kondo, Ichii, Patra, Canadell, et al. (2018) and Kondo et al. (2020).

3. Results

3.1. Contrasting Transitions of Net LUC Flux

First, we need to understand whether the existing estimates of the net LUC flux (− for a net sink on land and + for a net source) agree in having a consistent pattern of spatiotemporal variability. Spatial patterns of decadal mean net LUC flux by the TRENDY v2 ensemble, v7 ensemble, H&N, and BLUE consistently showed that most parts of insular and continental Southeast Asia were a net source of CO_2 for the period 1980s−2000s (Figure 1a). However, their temporal variability was found to differ among estimates (Figures 1b and 1c). According to the TRENDY v2 ensemble, the net LUC flux gradually increased from the 1980s to 1990s, then decreased in the 2000s, while the net LUC flux of the TRENDY v7 ensemble decreased from the 1980s to 1990s, then increased through the 2000s and 2010s (Figure 1b). H&N showed temporal variability of the net LUC flux resembling the pattern of the TRENDY v2 models, but with a more notable emission increase in the 1990s and an emission decrease in the 2000s (Figure 1c). Conversely, BLUE showed a pattern of the net LUC flux consistent with the TRENDY v7 ensemble.

We further investigated individual patterns of the 10 DGVMs from TRENDY v2 and v7. Visually, the degree of similarity and dissimilarity in temporal variability of the net LUC flux between TRENDY v2 and v7 largely varied depending on DGVMs (Figure 2). For instance, a difference between the two versions was notable in CLM, LPJ-wsl, O-CN, and VISIT, particularly for the 1990s, while it appears insignificant in JULES, and LPX-Bern. These could be caused by differences in forest distributions, biomass estimates, emissions factors, and schemes of LUC models among DGVMs (Arneth et al., 2017; Calle et al., 2016). However, when the difference in interannual variability between TRENDY v2 and v7 was normalized (i.e., normalized$[v2-v7]_i$ = ($[v2-v7]_i$ – mean$[v2-v7]$)/ standard deviation$[v2-v7]$, i = 1980–2012, positive values representing greater LUC emissions in v2 than v7, and vice versa), it became evident that the pattern of v2 having greater LUC emissions for the 1990s than v7 is common within all the DGVMs (Figure 2).

Summarizing the comparison of the independent estimates of the net LUC flux leads to two different scenarios of historical LUC transition for Southeast Asia.

Scenario 1 (TRENDY v2 and H&N): Southeast Asia experienced an active period of LUC during the 1980s−1990s, and after having a peak in the 1990s, LUC emissions were stabilized or even decreased in the 2000s, more so in the 2010s.
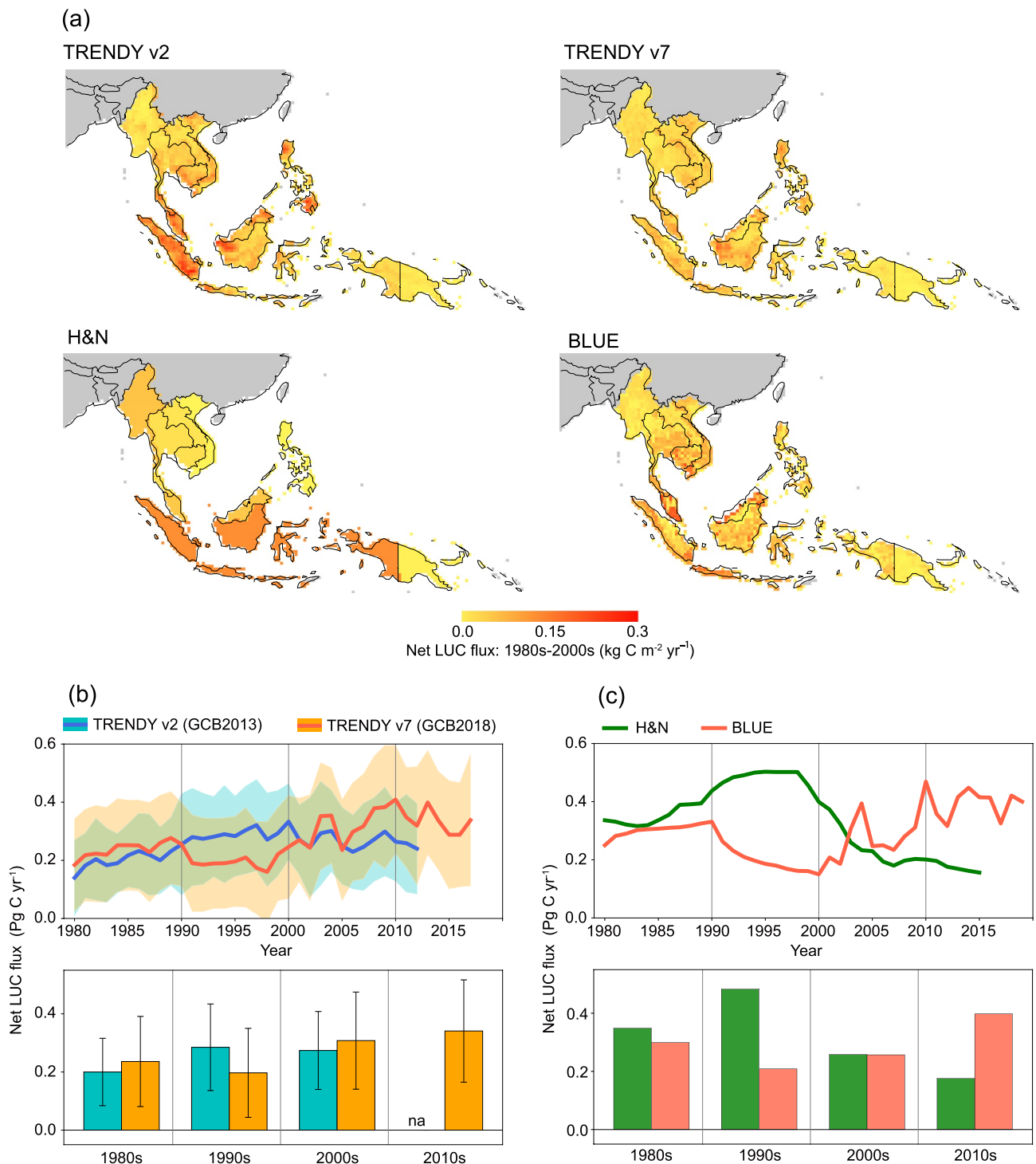
Scenario 2 (TRENDY v7 and BLUE): Southeast Asia experienced declining LUC emissions from the 1980s to the 1990s, and intensifying LUC emissions through the 2000s and 2010s.

To identify which of these scenarios is more likely, we need to identify a plausible trend in LUC transitions focusing on the 1990s.

3.2. Causes Behind the Contrasting LUC Transitions

We investigated whether the updates of the LUC forcing (HYDE and LUH) are related to contrasting estimates of the net LUC flux for Southeast Asia. In both the v3.1 and v3.2 of HYDE, the sum of cropland and pasture area continuously increased for the 1980s−2010s (Figure 3a), of which cropland accounts most (Figures 3b and 3c). HYDE v3.1 and v3.2 closely resemble each other in the pattern of temporal variability where cropland and pasture areas increased from 1980 to 1990. Between those periods, the net area increase was greater in the v3.1 than the v3.2 by approximately 1 million ha (Figure 3a). This implies that, when used to force DGVMs, HYDE v3.1 induces a slightly greater loss of ecosystem land cover (including forest, grass, and shrub) for the 1990s than the v3.2.

The sum of primary and secondary land areas (comprised of forest and non-forest) of LUH v1 and v2 commonly showed a continued decrease for the 1980s−2010s, with a slightly greater rate of area loss in the v1 than v2 during the 1990s (approximately 3 million ha, Figure 3d). Despite the similarity in their sum, primary and secondary land areas were largely different between the two versions. In LUH v1, primary land area showed 18 million

Figure 1. Spatiotemporal variability in the net land-use changes (LUC) flux of the TRENDY v2 and v7 ensembles and book-keeping models. (a) Spatial variability in mean net LUC flux for the 1980s−2000s estimated by the TRENDY v2 model ensemble, v7 model ensemble, H&N, and BLUE for Southeast Asia. Interannual and decadal variability in the net LUC flux by (b) the TRENDY v2 and v7 ensembles, and (c) H&N and BLUE. Shades and error bars in (b) represent 1σ spread from the mean value of the TRENDY ensemble.
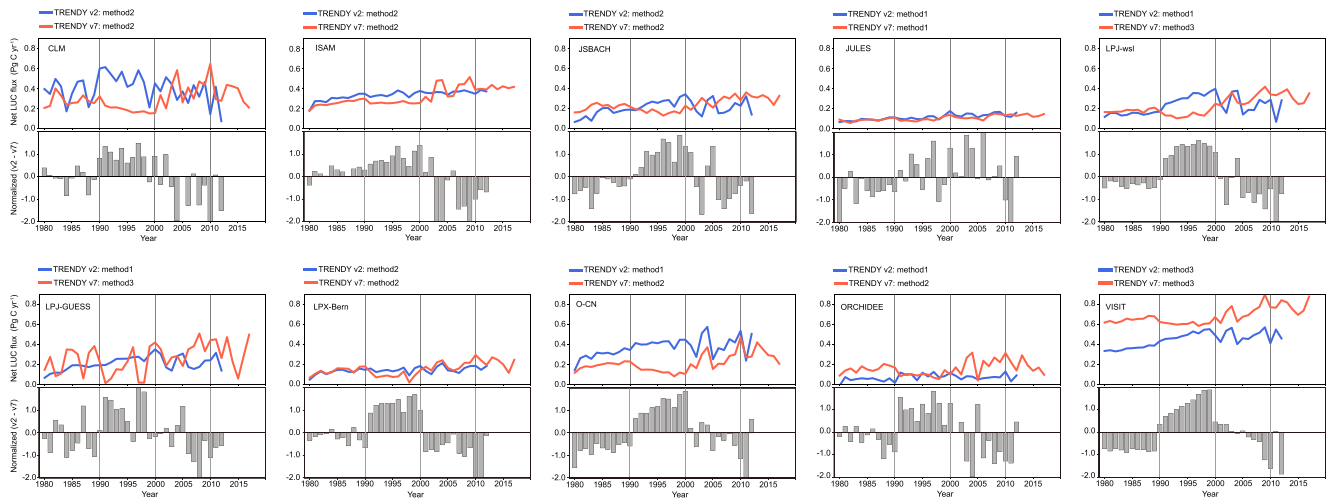
Figure 2. Temporal variability in the net land-use changes (LUC) flux by individual TRENDY v2 and v7 models. Interannual variability in the net LUC flux of the 10 Dynamic Global Vegetation Models (CLM, ISAM, JSBACH, JULES, LPJ-wsl, LPJ-GUESS, LPX-Bern, O-CN, ORCHIDEE, and VISIT) is shown along with a normalized difference between TRENDY v2 and v7.

ha loss between 1990 and 2000 (Figure 3e) and a corresponding 12 million ha gain in secondary land area for the same period (Figure 3f). In contrast, in LUH v2, both the loss of primary land area and gain of secondary land area in the 1990s reduced from those in LUH v1 by 33%–39%, making the LUC transition from primary to secondary land in the 1990s less significant (Figures 3e and 3f). Isolating components of primary and secondary lands further, we found that the major difference between LUH v1 and v2 was in forest area (Figures 3g–3i). A 17 million ha loss of primary forest area between 1990 and 2000 in LUH v1 reduced to a 10 million ha loss in
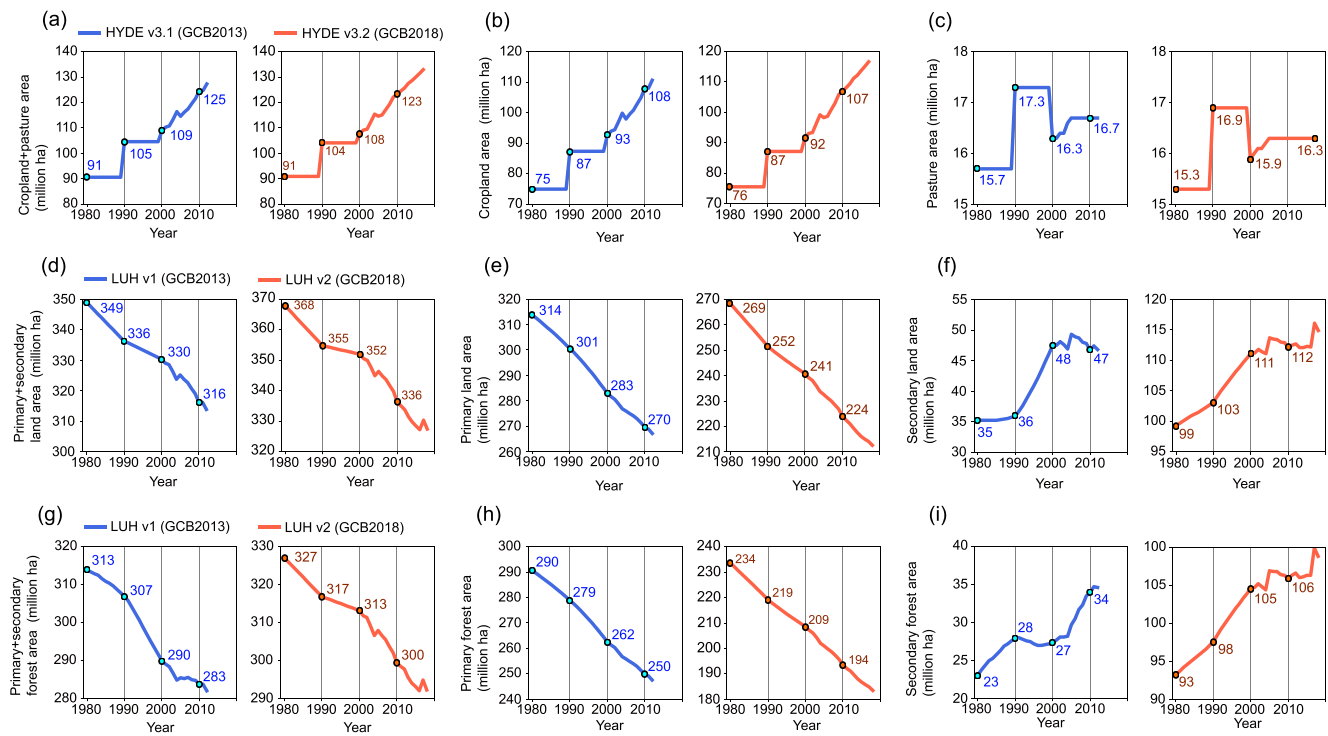

Figure 3. Temporal variability in cropland, pasture, primary and secondary lands, and primary and secondary forests defined in the land-use changes forcing data (HYDE and LUH). Interannual variability in the older and newer versions of HYDE (HYDE v3.1 and v3.2) and LUH (LUH v1 and v2) is shown for (a) cropland + pasture, (b) cropland, (c) pasture, (d) primary + secondary land, (e) primary land, (f) secondary land, (g) primary + secondary forest, (h) primary forest, and (i) secondary forest, for 1980–2017.
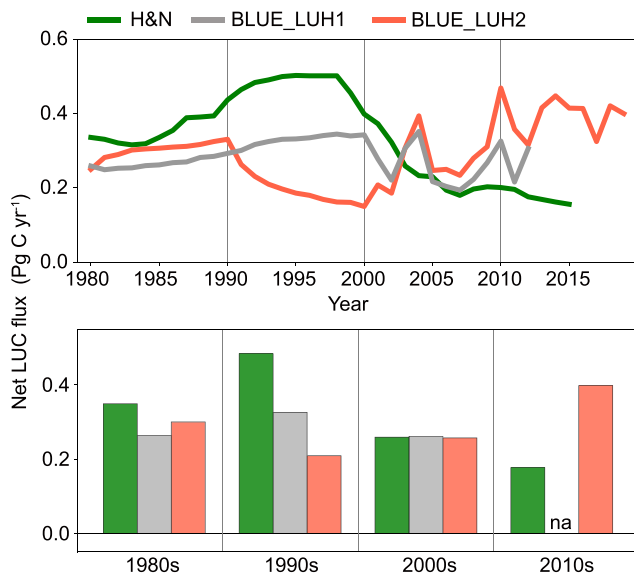
Figure 4. Reassessment of temporal variability in the net land-use changes (LUC) flux of the book-keeping models. Interannual and decadal variability in the net LUC flux by H&N and the two BLUE simulations forced by LUH v1 and LUH v2 (BLUE_LUH1 and BLUE_LUH2, respectively). Other configurations are the same as in Figure 1c.

LUH v2 (Figure 3h). For the same period, secondary forest area was almost unchanged in LUH v1 (the change affects secondary non-forest area instead; Figure S2 in Supporting Information S1), while it increased by 7 million ha in LUH v2 (Figure 3i). As a result, a loss of total forest area (a sum of primary and secondary forest area) between 1990 and 2000 was four-fold greater in LUH v1 than v2 (Figure 3g).

Our evaluation of the LUC forcing data revealed that the older forcing data (HYDE v3.1 and LUH v1) yielded a greater ecosystem loss for the 1990s than the newer ones (HYDE v3.2 and LUH v2), and it is expected to impact the net LUC flux simulations of DGVMs. For DGVMs that based their LUC modeling on the distinguished transition approach (the method 3: VISIT) or changed the modeling base from the summed transitions to the distinguished transitions (from the method 1 to method 3: LPJ-GUESS and LPJ-wsl), decadal transitions of the net LUC flux tended to produce greater emissions for the 1990s in TRENDY v2 than v7 (Figure 2). A similar pattern was found for those that changed the modeling base from method 1 to method 2 (O-CN, and ORCHIDEE) or explicitly based on method 2 (CLM, ISAM, JSBACH, and LPX-Bern), although it stood out less in LPX-BERN (Figure 2). For the DGVM that based the LUC modeling on method 1 (JULES), differences were even smaller, but a similar pattern was found through normalization (Figure 2).

The difference in the net LUC flux between the two book-keeping models may also be related to the data they used. H&N based its estimate directly on the FAO and FRA national statistics, which indicates a notable peak of forest loss in the 1990s for Southeast Asia (FAO, 2015; FAO, 2020). On the other hand, BLUE based its estimation on the distinguished transition approach using LUH v2, in which a forest loss peak did not stand out in the 1990s, as shown in Figures 3g–3i. To elaborate on the influence of forcing data on the net LUC flux, we compared two BLUE simulations forced by LUH v1 (BLUE_LUH1) and v2 (BLUE_LUH2) with the same model configuration. Although the magnitude of decadal changes is still different, the net LUC flux by BLUE_LUH1 showed an increase in LUC emissions from the 1980s to 1990s and a decrease in the 2000s as in H&N (Figure 4), indicating that the update of forcing data is responsible for the emissions difference between the older and newer estimates of net LUC flux.

Figure 5 shows a summary of decadal changes in the net LUC flux between the TRENDY v2 and v7 simulations, and in ecosystem gain and loss due to changes in the LUC modeling approaches. It is evident that the older set of LUC forcing data and TRENDY simulations yields a greater ecosystem loss and corresponding higher emissions for the 1990s than the newer one, and this result is supported by similar trends using LUH v1 versus LUH v2 in BLUE. The key finding here is that the difference in the net LUC flux between the two TRENDY versions consistently occurred in the 1990s regardless of choice (HYDE or LUH) and model implementation of LUC forcing data (summed or distinguished approach) among the DGVMs (Figure 5). These results indicate that the underlying LUC forcing data are more important in reproducing the trend in flux than the type of model used to calculate it. The climate forcing was also changed between TRENDY v2 and v7 (from CRU-NCEP to CRU-JRA). Still, their difference is unlikely responsible for contrasting net LUC flux estimates. Spatiotemporal variability in air temperature, precipitation, and short-wave radiation for Southeast Asia is similar between CRU-NCEP and CRU-JRA without a notable difference between decades, in contrast to the LUC forcing data (Figure S3 in Supporting Information S1).

4. Discussion

4.1. Evaluation of the Two Scenarios

We considered sources of modeled difference behind the two different scenarios about the historical LUC transition of Southeast Asia. To identify which scenario better reflects a realistic transition, we discuss the plausibility
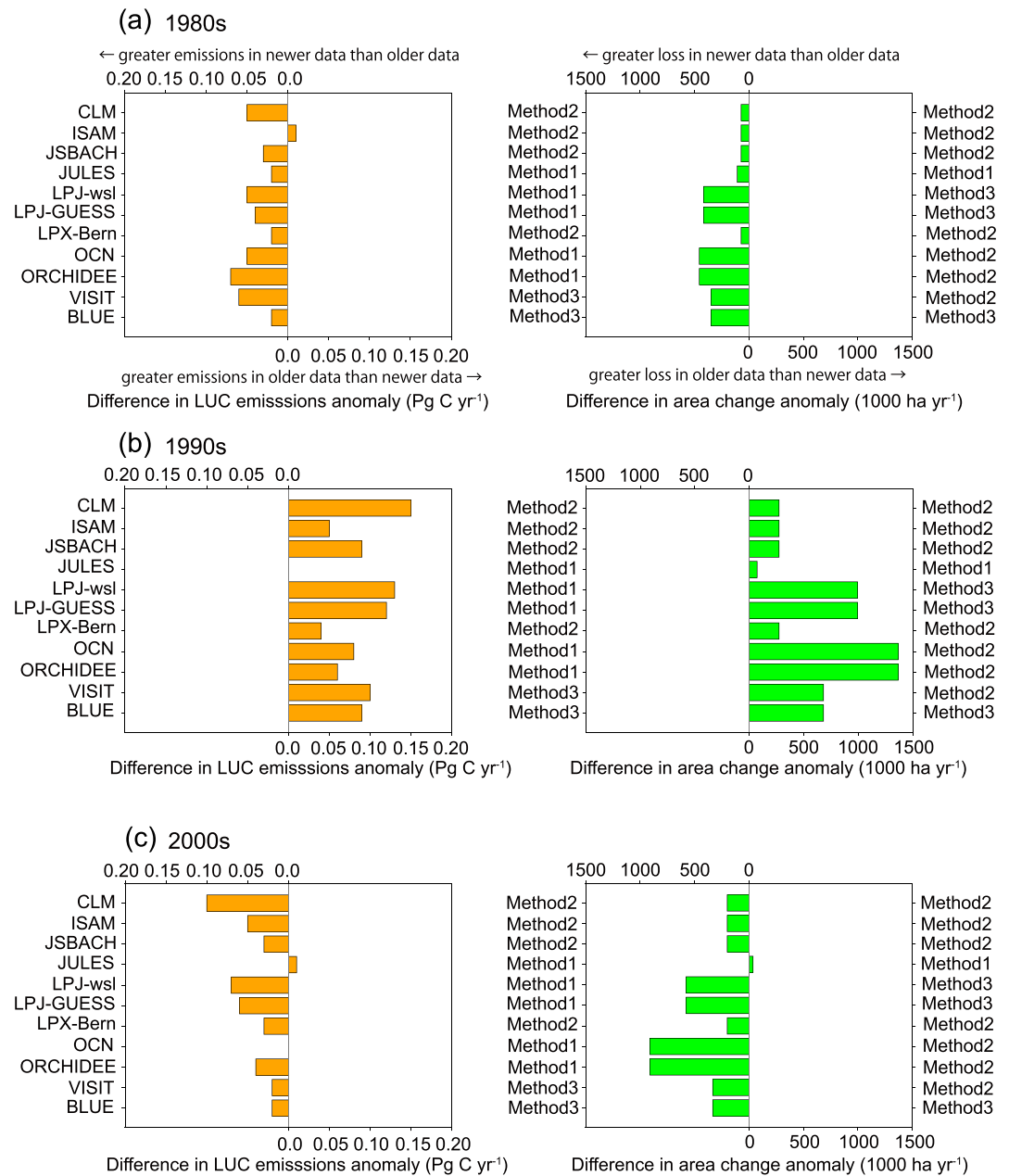
Figure 5. Summary of decadal patterns of the net land-use changes (LUC) flux by TRENDY v2 and v7 and forcing data used for the TRENDY simulations. Differences in the net LUC flux anomaly between TRENDY v2 and v7 and in area change anomaly between the LUC forcing data used for running those simulations (HYDE v3.1, v3.2, LUH v1, and v2) for (a) the 1980s, (b) 1990s, and (c) 2000s. The base period for anomaly is 1980–2009. Differences in area change anomaly between the older and newer forcing data are set as follows: method1 to method1 (differences in ecosystem area change anomaly between HYDE v3.1 and v3.2), method2 to method2 (differences in primary + secondary land area change anomaly between LUH v1 and v2), method3 to method3 (differences in primary land area change anomaly between LUH v1 and v2), method1 and method2 (differences between ecosystem area change anomaly from HYDE v3.1 and primary + secondary land area change anomaly from LUH v2), and method1 and method3 (differences between ecosystem area change anomaly from HYDE v3.1 and primary land area change anomaly from LUH v2). Ecosystem area represents an area that inversely corresponds to cropland + pasture area change from HYDE (e.g., gain of cropland + pasture area corresponds loss of ecosystem area, and vice versa).
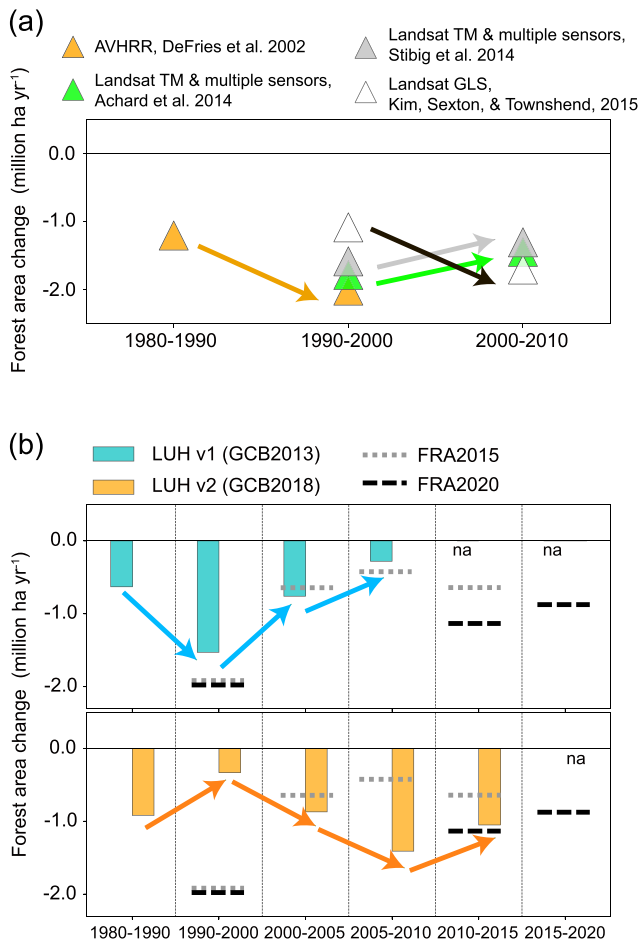
Figure 6. Decadal forest area changes in Southeast Asia. Decadal changes in forest area estimates by (a) literature values from four remote sensing studies (Achard et al., 2014; DeFries et al., 2002; Kim et al., 2015; Stibig et al., 2014) and (b) by LUH v1 and v2 (a sum of primary and secondary forest), and FRA2015 and 2020.

of historical LUC transition through independent data and analyses based on forest area changes from remote sensing studies, atmospheric inversions, and the history of forestry and environmental policies, respectively.

4.1.1. Forest Area

Forest area is the key proxy for LUC transitions in tropical regions. Several studies have assessed spatially explicit forest area over the Southeast Asian region using various remote sensing sensors, such as AVHRR, Landsat series, RapidEye, AVNIR, Kompsat, Demos, and MODIS (e.g., Achard et al., 2002, 2004, 2014; DeFries et al., 2002; Hansen et al., 2008, 2009, 2013; Kim et al., 2015; Mayaux et al., 2005; Stibig et al., 2014). Evaluating estimates that extend over two decades (Figure 6a), we found that forest loss in Southeast Asia increased from 1980–1990 to 1990–2000 (DeFries et al., 2002) and decreased from 1990–2000 to 2000–2010 (Achard et al., 2014; Stibig et al., 2014). These studies indicate that forest loss peaked in 1990–2000 over the past decades. At finer scales, the LUH forest area is not directly comparable with forest cover products such as those from remote sensing data due to differences in the underlying definition of forest cover. However, in Southeast Asia as a whole, the consistency in decadal forest area changes among LUH v1, remote sensing studies, and national statistics (FRA 2015 and 2020: FAO, 2015; FAO, 2020) supports the scenario in which there was the significant forest loss from the region in 1990–2000 (Figure 6b).

An exception to these results is a study based on Landsat Global Land Survey (Figure 6a), which indicated an increase in forest loss from 1990–2000 to 2000–2010 (Kim et al., 2015). Achard et al. (2014), Stibig et al. (2014), and Kim et al. (2015) all based their estimates on the Landsat series, but they resulted in contrasting decadal forest area changes. Differences in data processing likely contribute to those contrasting results. Kim et al. (2015) estimated forest cover between 2000 and 2005. Then, they used stable pixels identified in 2000 and 2005 to extent forest cover estimates for the years 1990 and 2010. In this approach, forest area changes are biased with higher estimates for the 2000s compared to the 1990s because using the two sub-periods of six-year duration (i.e., 2000–2005 and 2005–2010) captures parts of the short-time visible removals of tree cover in 2005. In contrast, although methodology details differ, Achard et al. (2014) and Stibig et al. (2014) commonly processed data of the two decades with consistent temporal approaches.

It should be noted that a transition of forest area estimated by remote sensing account for the effect of both anthropogenic and natural disturbances. However, despite a relatively large amount of CO_2 emissions, natural disturbances, such as biomass burning tend to be localized events in Southeast Asia. For instance, even the phenomenal biomass burning in the 1997/1998 El Niño episode resulted in a burnt area of 0.75 million ha over Southeast Asia, amounting to 36% of the 2.11 million ha forest loss between 1990 and 2000 (FAO, 2015). Therefore, it is reasonable to assume that a major part of decadal forest area changes in Southeast Asia observed by remote sensing originated in LUC activities as suggested by previous studies that assessed land cover changes in Southeast Asia (e.g., Achard et al., 2014; DeFries et al., 2002; Hansen et al., 2013; Stibig et al., 2014).

4.1.2. Net Terrestrial CO_2 Flux

Next, we compared decadal variability in the net CO_2 flux (total CO_2 balance accounting for the effects of CO_2 fertilization, climate, and LUC) of the TRENDY v2 and v7 models with the atmospheric inversions. We found that for the TRENDY v2 models, the net CO_2 fluxes are overall a net source of CO_2 for the 1980s−1990s, having the peak net emissions in the 1990s driven by LUC (Figure 7). In turn, the net source in the 1990s shifted towards a net sink in the 2000s, as an increased CO_2 uptake by the effects of CO_2 fertilization and climate variability (CO_2 + climate effect) reduced LUC emissions. On the other hand, the net CO_2 fluxes of the TRENDY v7 models show decadal changes that are stable or slightly increased towards a net sink between the 1980s and 1990s, reflecting
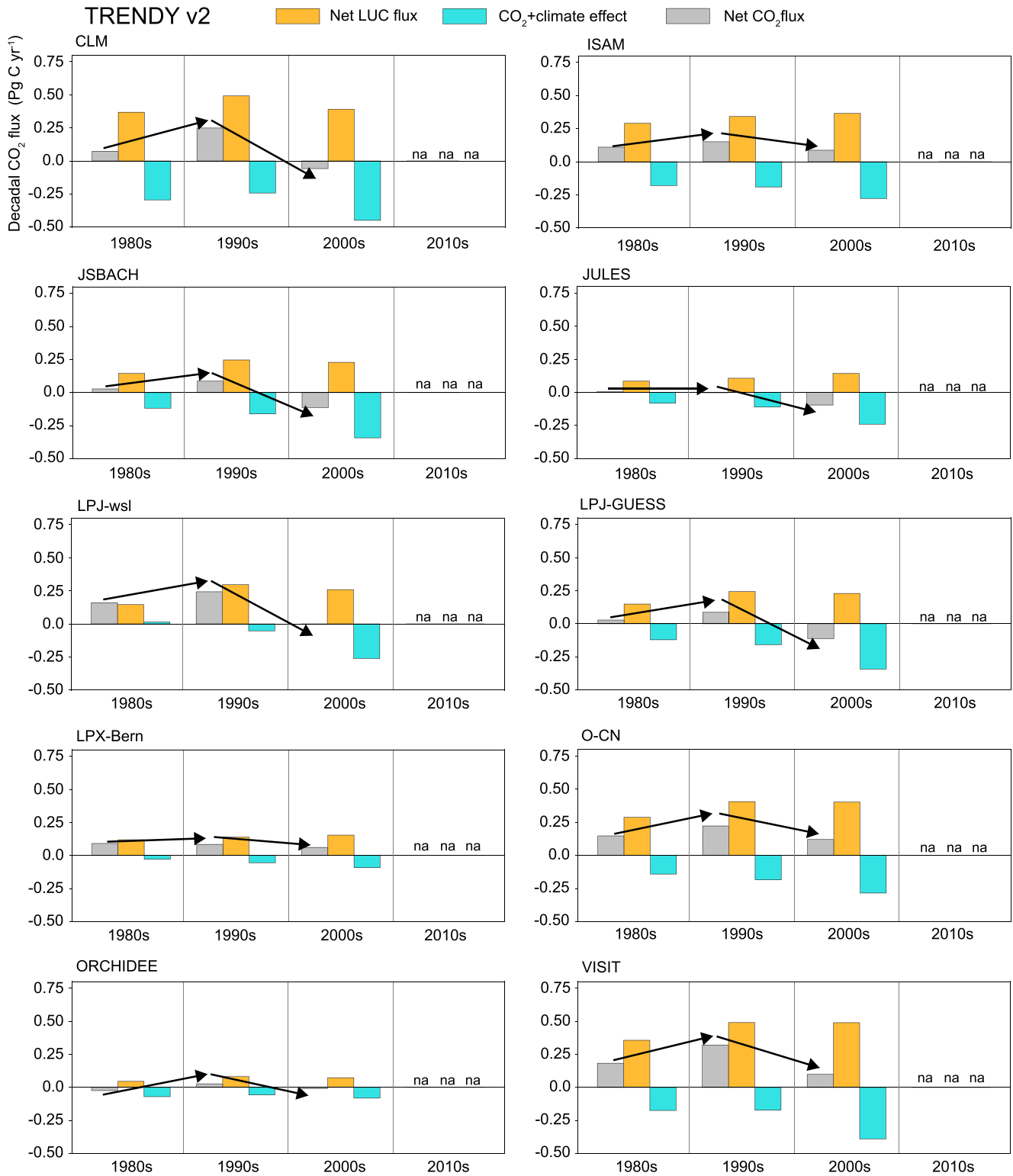
Figure 7. Decadal variability in the net CO_2 flux and component fluxes for Southeast Asia estimated by the TRENDY v2 simulations. Decadal variability in the net CO_2 flux (gray bars), the CO_2 + climate effect (cyan bars) and land-use changes (LUC) effect (net LUC flux: orange bars) on the net CO_2 flux. Results are shown for individual models from TRENDY 2. Arrows indicates decadal changes in the net CO_2 flux.

the change in the net LUC flux (Figure 8). Then, they shifted towards a net source in the 2000s or 2010s, depending on models. These results indicate that the net LUC flux significantly controls decadal variability in the net CO_2 flux for Southeast Asia revolving around the 1990s, as previously suggested by Kondo, Ichii, Patra, Canadell, et al. (2018). In addition, as in the case of the net LUC flux (Figure 2), the normalized difference in the net CO_2 flux between TRENDY v2 and v7 showed that the pattern of v2 having greater net emissions for the 1990s than v7 is common within all the DGVMs (Figure S4 in Supporting Information S1). These results indicate that examining independent estimates of the net CO_2 flux serves as an indirect evaluation of the historical LUC transition.

The three atmospheric inversions (ACTM, JMA, and NICAM-TM) exhibited a decadal shift from a strong to reduced net source between the 1990s and 2000s (Figure 9), similar to the pattern shown by TRENDY v2. This result held even when the 1997/1998 period, where the phenomenal biomass burning occurred due to the 1997/98 El Niño event, was excluded from the decadal mean. Thus, it indicates that biomass burning associated with the 1997/98 El Niño episode alone is not responsible for the peak of net CO_2 emissions found in the 1990s. Instead, it suggests that the contribution of LUC to the more positive CO_2 flux anomaly during the 1990s compared with the 2000s is driving the trend.

4.1.3. History of Forestry and Environmental Policy

Our evaluation of remote sensing studies and atmospheric inversions suggested the occurrence of peak LUC activities and emissions in the 1990s instead of the 2000s or 2010s, favoring the historical LUC transition of scenario 1. The history of forestry and environmental policy making in Southeast Asian countries supports this result. Since the 1960s, natural forests in Southeast Asian countries have been a major resource for timber production, especially in Philippines, Thailand, and Viet Nam during the 1960s−1980s, and in Malaysia and Indonesia during the 1980s−1990s (FAO, 2011, 2015). According to "the FAO Southeast Asian forests and forestry to 2020" (FAO, 2011), Southeast Asia's period of active forestry reversed mainly due to the following factors; (a) several countries (e.g., Philippines, Thailand, and Viet Nam) commenced the regulation of timber production and national-level afforestation and reforestation programs in parallel (FAO, 2011), (b) the 1997/1998 Asian economy crisis caused a significant decrease in wood products production (Broadhead, 2006), and most importantly (c) the economic focus of Southeast Asian countries has shifted from timber production to plantation including sawlogs, pulpwood, bioenergy, and rubber productions (wood production market began to shift from Indonesia and Malaysia to Southern countries, e.g., New Zealand, Australia, Chile, and South Africa: FAO, 2011). These events in conjunction most likely led to the recovery of forest area (including an increase in conservation and protected forests and plantations) in the 2000s and are thus responsible for the LUC transition between the 1990s and 2000s.

In contrast, the LUC transition suggested by scenario 2 is not in line with the past and current historical events. To the best of our knowledge, there is no historical event or ratified government and international policies supporting the decrease in LUC emissions over Southeast Asia from the 1980s to the 1990s. Also, a persistent increase in LUC emissions after 2000, another feature of scenario 2, runs counter to the 2000s being a decade that forest protection awareness has increased, leading to the ratification of REDD+ and establishment of more than 50 REDD + type projects in Southeast Asian countries (Ziegler et al., 2012).

4.2. Uncertainty in LUC Forcing and Modeling

Our results support the plausibility of scenario 1: the decadal LUC transition characterized by the peak LUC emissions in the 1990s as indicated by the older simulations (ran with the older forcing data). The two versions of HYDE are closely consistent in transitions of cropland and pasture areas, and correspondingly the influences on the net LUC flux are small (as illustrated by the result of JULES: Figure 2). However, differences in the two versions of LUH, particularly forest transitions, are notable; thus, they are largely responsible for the contrasting net LUC flux transitions between TRENDY v2 and v7.

In the scheme of LUH v1, primary land was used as a priority for wood harvest and land conversion demanded by agriculture, both based on the FAO statistics (Hurtt et al., 2006). Therefore, in LUH v1, the decrease in primary land in the 1990s, of which primary forest accounts most, corresponds to the increased cropland (agricultural demand) and secondary non-forest vegetation (due to wood harvest) (Figures 3a and 3e, and Figure S2e in Supporting Information S1). However, in LUH v2, these patterns changed primarily due to the difference in forest transitions between LUH v1 and v2. The decrease in primary forest is less pronounced (Figure 3h), and secondary
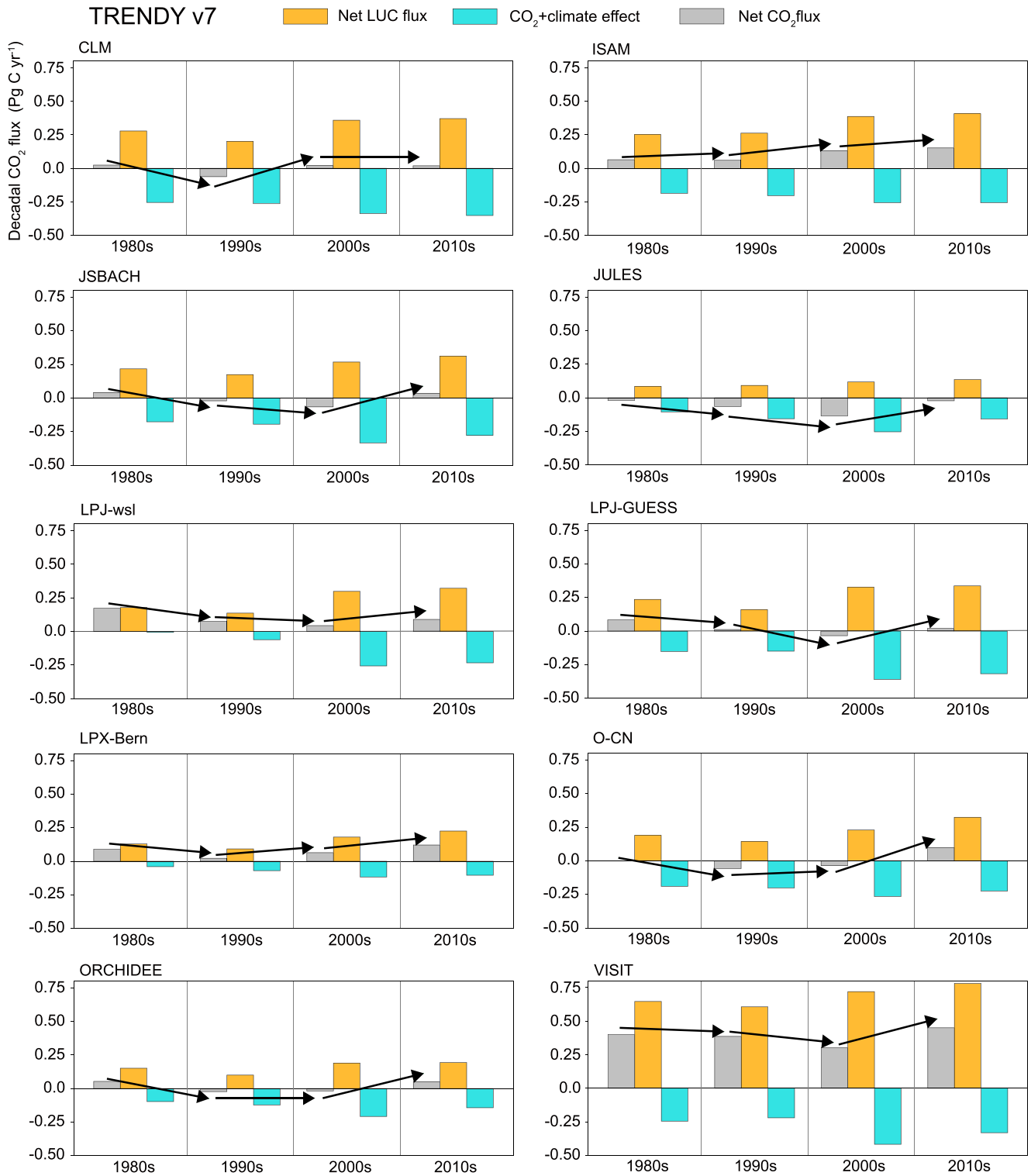
Figure 8. Decadal variability in the net CO_2 flux and component fluxes for Southeast Asia estimated by the TRENDY v7 simulations. Decadal variability in the net CO_2 flux (gray bars), the CO_2 + climate effect (cyan bars) and land-use changes (LUC) effect (net LUC flux: orange bars) on the net CO_2 flux. Results are shown for individual models from TRENDY 7. Arrows indicates decadal changes in the net CO_2 flux.
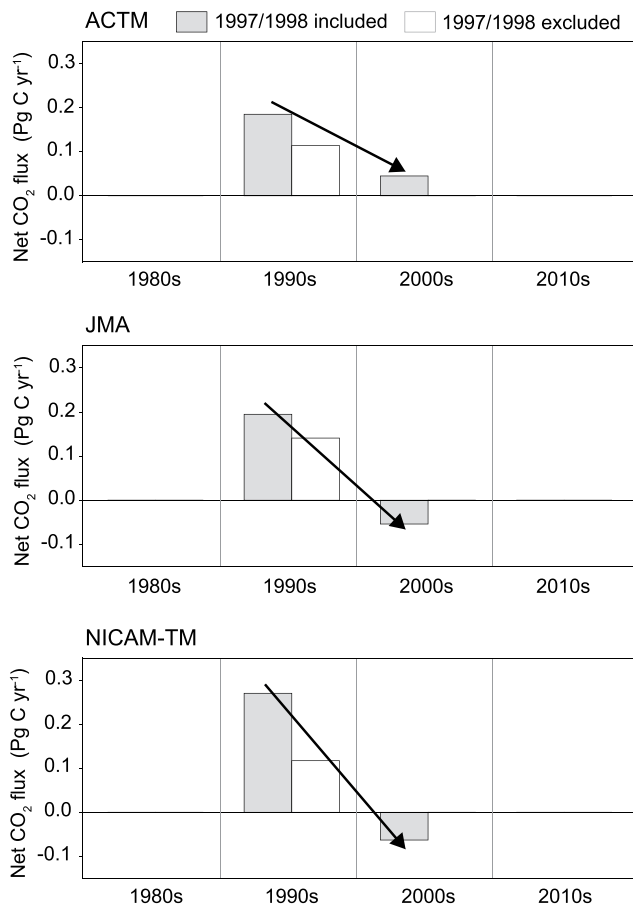
Figure 9. Decadal variability in the net CO_2 flux from three atmospheric inversions for Southeast Asia. Decadal variability in the net CO_2 flux by ACTM, JMA, and NICAM-TM. Decadal CO_2 budget of these atmospheric inversions for the 1990s are shown with and without the 1997/1998 value.

forest increased instead of secondary non-forest vegetation (Figure 3i). Considering the changes between the LUH versions, a newly implemented satellite-based constraint on the spatial patterns of forest transitions may be responsible for the difference in forest transitions between the LUH versions (Figures 3g and 6b). Because of a relatively simple design, forest transitions in LUH v1 more directly reflect the FAO statistics used as a basis, whereas those in LUH v2 possibly reflect the FAO statistics less due to increased constraints, including forest transitions.

Yet, it does not necessarily imply that the older versions of LUC forcing are more reliable than the newer versions. Examining spatial variability in the LUC forcing data, decadal changes in cropland of HYDE v3.1 and secondary land in LUH v1 for the period 1990–2000 are rather heterogeneous to be realistically compared with those of HYDE v 3.2 and LUH v2 (Figure 10). The spatialization method using remote sensing data successfully smoothed out spatial variability in the newer forcing data (Figure 10). In sum, although our results support the plausibility of scenario 1, both the older and newer versions of LUC forcing have issues of their own, and both smoothed spatial patterns and preservation of the regional FAO value need to be realized in future forcing data. Lastly, we emphasize that our results on the LUC forcing data are only valid for Southeast Asia and the period analyzed. It should not be extended to other regions without detailed analyses as done in this study.

To understand whether LUC emissions continue to decline after the 2000s, we need to address the uncertainty associated with incomplete processes in the LUC forcing data and modeling for Southeast Asia. A land-cover conversion of peatland to oil-palm plantation is the key process relevant to the recent net LUC flux for Southeast Asia, but not represented in the LUC forcing data. CO_2 emissions following clear-cutting peat forests and drainage of peat swamps contribute significantly to the carbon budget in Southeast Asia and the global total (Uryu, 2008). It is known that oil-palm plantation is directly responsible for 40% to 62% of those peatland disturbances (Carlson et al., 2012, 2018; Murdiyarso et al., 2010). Today, information on peatland is yet to be a part of the FAO data and LUH, and oil-palm plantation is not explicitly categorized in neither the FAO data nor HYDE (they are implicitly included in cropland of those data). Likewise, biogeochemical modeling for this LUC type is still under development. To our knowledge, CLM is the only model that attempted to model fire emissions from peatland (Li et al., 2013; 2014) and the carbon cycle in oil-palm ecosystems (Fan et al., 2015; Meijide et al., 2017). However, many issues remain in its modeling, such as not considering the temporal changes of peatland cover, a lack of CO_2 emissions from peat oxidation, and incomplete parameterization for the carbon cycle of the oil-palm ecosystem. Under the circumstance where the increase in oil-palm plantation at the expense of peat forest does not seem to stop today, the implementation of peatland to oil-palm land-cover change in LUC forcing and sophisticated modeling for this LUC transition in DGVMs are expected to play a critical role in the net LUC flux estimation for today and future.

Furthermore, despite progress towards more sophisticated representations of LUC modeling, further efforts to reduce differences in LUC modeling are strongly needed. In addition to the LUC modeling approach (summed or distinguished transition), implementation of wood and crop harvests, consideration of residue carbon after deforestation, and turnover rates of a product pool are still largely different among DGVMs (Le Quéré, Andrew, Friedlingstein, Sitch, Pongratz, et al., 2018; Le Quéré, Andrew, Friedlingstein, Sitch, Hauck, et al., 2018). These various schemes of LUC modeling induce non-negligible differences in estimates of the net LUC flux, not only for Southeast Asia (Figure 2, Calle et al., 2016), but also for the global land (Arneth et al., 2017). A comparison of LUC modeling is currently in progress as part of the Coupled Model Intercomparison Project (CMIP): namely the Land Use Model Intercomparison Project: LUMIP (Lawrence et al., 2016). However, LUMIP is an experiment dedicated to identifying long-term effects and projections of LUC based on climate scenarios. We need an

Figure 10. Spatial patterns of decadal ecosystem area changes in Southeast Asia. Spatial variability in changes of (a) cropland, (b) pasture, (c) primary land, and (d) secondary land, between 1990 and 2000. Estimates of HYDE v3.1, HYDE v3.2, LUH v1, and LUH v2 are shown. In each plot, an inset shows a histogram of area change distribution.

experiment aimed explicitly at the contemporary period (e.g., 1980–current) to develop a more realistic LUC modeling reflecting information from available observations and national statistics.

5. Conclusions

This study detailed the net LUC flux estimates to identify a plausible historical LUC transition for Southeast Asia. The key message from this study is that there is a substantial amount of uncertainty in our assessments of net LUC flux primarily rooted in forcing data. There is no guarantee that the newer data are of a better quality than the older ones. One should carefully evaluate available methods and estimates when assessing historical regional net LUC flux transitions because any assessment relying on a specific method or forcing data may lead to unrealistic results.

For Southeast Asia, the multiple independent evidence supports the plausibility of scenario 1: the LUC transition of the peak emissions in the 1990s to the declining emissions in the 2000s and beyond. Although the older forcing data have issues of their own (i.e., heterogeneous spatial variability), this scenario itself should be regarded as most realistic as supported by the independent analyses and data. Thus, it should be reproduced in a new estimate and be the base for future improvements of net LUC flux (e.g., land cover change from peatland to oil-palm plantation), which is anticipated in the on-going project of carbon budget assessment for Southeast Asia under REgional Carbon Cycle Assessment and Processes phase 2 (RECCAP2). A complete synthesis of carbon budget assessment supported by a new net LUC flux estimate is expected to shed light on the role of Southeast Asia in the global carbon cycle and the effectiveness of local and international policies on deforestation prevention for that region.

Conflict of Interest

The authors declare no conflicts of interest relevant to this study.

Data Availability Statement

TRENDY data for this research are available through Le Quéré, Andrew, Friedlingstein, Sitch, Hauck, et al. (2018), ACTM data are through Saeki and Patra (2017), NICAM-TM data are through Niwa et al. (2012), JMA inversion data are through Maki et al. (2010), H&N data are through Houghton and Nassikas (2017), and BLUE data are through Hansis et al. (2015), respectively.

References

Achard, F., Beuchle, R., Mayaux, P., Stibig, H.-J., Bodart, C., Brink, A., et al. (2014). Determination of tropical deforestation rates and related carbon losses from 1990 to 2010. *Global Change Biology*, *20*, 2540–2554. https://doi.org/10.1111/gcb.12605

Achard, F., Eva, H. D., Mayaux, P., Stibig, H.-J., & Belward, A. (2004). Improved estimates of net carbon emissions from land cover change in the tropics for the 1990s. *Global Biogeochemical Cycles*, *18*, 11. https://doi.org/10.1029/2003gb002142

Achard, F., Eva, H. D., Stibig, H.-J., Mayaux, P., Gallego, J., Richards, T., & Malingreau, J.-P. (2002). Determination of deforestation rates of the world's humid tropical forests. *Science*, *297*, 999–1002. https://doi.org/10.1126/science.1070656

Arneth, A., Sitch, S., Pongratz, J., Stocker, B. D., Ciais, P., Poulter, B., et al. (2017). Historical carbon dioxide emissions caused by land-use changes are possibly larger than assumed. *Nature Geoscience*, *10*, 79–84. https://doi.org/10.1038/ngeo2882

Baccini, A., Walker, W., Carvalho, L., Farina, M., Sulla-Menashe, D., & Houghton, R. A. (2017). Tropical forests are a net carbon source based on aboveground measurements of gain and loss. *Science*, *358*, 230–234. https://doi.org/10.1126/science.aam5962

Brando, P. M., Paolucci, L., Ummenhofer, C. C., Ordway, E. M., Hartmann, H., Cattau, M. E., et al. (2019). Droughts, wildfires, and forest carbon cycling: A pantropical synthesis. *Annual Review of Earth and Planetary Sciences*, *47*, 555–581. https://doi.org/10.1146/annurev-earth-082517-010235

Broadhead, J. S. (2006). *Asia-pacific forestry: Outlook and realities 5 years since APFSOS*. Retrieved from ftp://ftp.fao.org/docrep/fao/009/ah230e/ah230e00.pdf

Butler, J. H. (1980). *Economic geography: Spatial and environmental aspects of economic activity*. John Wiley.

Calle, L., Canadell, J. G., Patra, P., Ciais, P., Ichii, K., Tian, H., et al. (2016). Regional carbon fluxes from land use and land cover change in Asia, 1980–2009. *Environmental Research Letters*, *11*, 074011. https://doi.org/10.1088/1748-9326/11/7/074011

Carlson, K. M., Curran, L. M., Ratnasari, D., Pittman, A. M., Soares-Filho, B. S., Asner, G. P., et al. (2012). Committed carbon emissions, deforestation, and community land conversion from oil palm plantation expansion in West Kalimantan, Indonesia. *Proceedings of the National Academy of Sciences of the United States of America*, *109*, 7559–7564. https://doi.org/10.1073/pnas.1200452109

Carlson, K. M., Heilmayr, R., Gibbs, H. K., Noojipady, P., Burns, D. N., Morton, D. C., et al. (2018). Effect of oil palm sustainability certification on deforestation and fire in Indonesia. *Proceedings of the National Academy of Sciences of the United States of America*, *115*, 121–126. https://doi.org/10.1073/pnas.1704728114

Clark, D. A. (2004). Sources or sinks? The responses of tropical forests to current and future climate and atmospheric composition. *Philosophical Transactions of the Royal Society of London, Series B*, *359*, 477–491. https://doi.org/10.1098/rstb.2003.1426

DeFries, R., Houghton, R. A., Hansen, M., Field, C., Skole, D. L., & Townshend, J. (2002). Carbon emissions from tropical deforestation and regrowth based on satellite observations for the 1980s and 90s. *Proceedings of the National Academy of Sciences of the United States of America*, *99*, 14256–14261. https://doi.org/10.1073/pnas.182560099

ESA. (2017). *Land cover CCI product user guide version 2*. Tech. Rep. Retrieved from maps.elie.ucl.ac.be/CCI/viewer/download/ESACCI-LC-Ph2-PUGv2_2.0.pdf

Fan, Y., Roupsard, O., Bernoux, M., Le Maire, G., Panferov, O., Kotowska, M. M., & Knohl, A. (2015). A sub-canopy structure for simulating oil palm in the Community Land Model (CLM-Palm): Phenology, allocation and yield. *Geoscientific Model Development*, *8*, 3785–3800. https://doi.org/10.5194/gmd-8-3785-2015

Food and Agriculture Organization (FAO). (2011). *Southeast Asian forests and forestry to 2020: Sub-regional report of the second Asia-Pacific forestry sector outlook study*. FAO.

Food and Agriculture Organization (FAO). (2015). *Global Forest Resources Assessment 2015: How have the world's forests changed?*

Food and Agriculture Organization (FAO). (2020). *Global forest resources assessment 2020: Main report*.

Friedlingstein, P., Jones, M. W., O'Sullivan, M., Andrew, R. M., Hauck, J., Peters, G. P., & Zaehle, S. (2019). Global carbon budget 2019. *Earth System Scientific Data*, *11*, 1783–1838.

Gaubert, B., Stephens, B. B., Basu, S., Chevallier, F., Deng, F., Kort, E. A., et al. (2019). Global atmospheric CO_2 inverse models converging on neutral tropical land exchange, but disagreeing on fossil fuel and atmospheric growth rate. *Biogeosciences*, *16*(1), 117–134. https://doi.org/10.5194/bg-16-117-2019

Grassi, G., House, J., Kurz, W. A., Cescatti, A., Houghton, R. A., Peters, G. P., et al. (2018). Reconciling global-model estimates and country reporting of anthropogenic forest CO_2 sinks. *Nature Climate Change*, *8*(10), 914–920. https://doi.org/10.1038/s41558-018-0283-x

Gurney, K. R., Law, R. M., Denning, A. S., Rayner, P. J., Baker, D., Bousquet, P., et al. (2002). Towards robust regional estimates of CO_2 sources and sinks using atmospheric transport models. *Nature*, *415*(6872), 626–630. https://doi.org/10.1038/415626a

Gurney, K. R., Law, R. M., Denning, A. S., Rayner, P. J., Baker, D., Bousquet, P., et al. (2003). TransCom 3 CO_2 inversion intercomparison: 1. Annual mean control results and sensitivity to transport and prior flux information. *Tellus Series B Chemical and Physical Meteorology*, *55*, 555–579. https://doi.org/10.3402/tellusb.v55i2.16728

Gurney, K. R., Law, R. M., Denning, A. S., Rayner, P. J., Pak, B. C., Baker, D., et al. (2004). Transcom 3 inversion intercomparison: Model mean results for the estimation of seasonal carbon sources and sinks. *Global Biogeochemical Cycles*, *18*, GB1010. https://doi.org/10.1029/2003gb002111

Hansen, M. C., Potapov, P. V., Moore, R., Hancher, M., Turubanova, S. A., Tyukavina, A., et al. (2013). High-resolution global maps of 21st-century forest cover change. *Science*, *342*, 850–853. https://doi.org/10.1126/science.1244693

Hansen, M. C., Stehman, S. V., Potapov, P. V., Arunarwati, B., Stolle, F., & Pittman, K. (2009). Quantifying changes in the rates of forest clearing in Indonesia from 1990 to 2005 using remotely sensed data sets. *Environmental Research Letters*, *4*, 034001. https://doi.org/10.1088/1748-9326/4/3/034001

Hansen, M. C., Stehman, S. V., Potapov, P. V., Loveland, T. R., Townshend, J. R. G., DeFries, R. S., et al. (2008). Humid tropical forest clearing from 2000 to 2005 quantified by using multitemporal and multiresolution remotely sensed data. *Proceedings of the National Academy of Sciences of the United States of America*, *105*, 9439–9444. https://doi.org/10.1073/pnas.0804042105

Hansis, E., Davis, S. J., & Pongratz, J. (2015). Relevance of methodological choices for accounting of land use change carbon fluxes. *Global Biogeochemical Cycles*, *29*, 1230–1246. https://doi.org/10.1002/2014gb004997

Heinimann, A., Mertz, O., Frolking, S., Egelund Christensen, A., Hurni, K., Sedano, F., et al. (2017). A global view of shifting cultivation: Recent, current, and future extent. *PLoS One*, *12*(9), e0184479. https://doi.org/10.1371/journal.pone.0184479

Hooijer, A., Page, S., Canadell, J. G., Silvius, M., Kwadijk, J., Wösten, H., & Jauhiainen, J. (2010). Current and future CO_2 emissions from drained peatlands in Southeast Asia. *Biogeosciences*, *7*, 1505–1514. https://doi.org/10.5194/bg-7-1505-2010

Houghton, R. A., & Nassikas, A. A. (2017). Global and regional fluxes of carbon from land use and land cover change 1850–2015. *Global Biogeochemical Cycles*, *31*, 456–472. https://doi.org/10.1002/2016gb005546

Huijnen, V., Wooster, M. J., Kaiser, J. W., Gaveau, D. L. A., Flemming, J., Parrington, M., et al. (2016). Fire carbon emissions over maritime Southeast Asia in 2015 largest since 1997. *Scientific Reports*, *6*, 26886. https://doi.org/10.1038/srep26886

Hurtt, G. C., Chini, L., Sahajpal, R., Frolking, S., Bodirsky, B. L., Calvin, K., et al. (2020). Harmonization of global land-use change and management for the period 850–2100 (LUH2) for CMIP6. *Geoscientific Model Development*, *13*, 5425–5464. https://doi.org/10.5194/gmd-13-5425-2020

Hurtt, G. C., Chini, L. P., Frolking, S., Betts, R. A., Feddema, J., Fischer, G., et al. (2011). Harmonization of land-use scenarios for the period 1500–2100: 600 years of global gridded annual land-use transitions, wood harvest, and resulting secondary lands. *Climate Change*, *109*, 117–161. https://doi.org/10.1007/s10584-011-0153-2

Hurtt, G. C., Frolking, S., Fearon, M. G., Moore, B., Shevliakova, E., Malyshev, S., et al. (2006). The underpinnings of land-use history: Three centuries of global gridded land-use transitions, wood-harvest, and resulting secondary lands. *Global Change Biology*, *12*, 1208–1229. https://doi.org/10.1111/j.1365-2486.2006.01150.x

Keenan, T. F., Prentice, I. C., Canadell, J. G., Williams, C. A., Wang, H., Raupach, M., & Collatz, G. J. (2016). Recent pause in the growth rate of atmospheric CO_2 due to enhanced terrestrial carbon uptake. *Nature Communications*, *7*, 13428. https://doi.org/10.1038/ncomms13428

Kim, D.-H., Sexton, J. O., & Townshend, J. R. (2015). Accelerated deforestation in the humid tropics from the 1990s to the 2000s. *Geophysical Research Letters*, *42*, 3495–3501. https://doi.org/10.1002/2014gl062777

Klein Goldewijk, K., Beusen, A., Doelman, J., & Stehfest, E. (2017). Anthropogenic land use estimates for the Holocene – HYDE 3.2. *Earth System Scientific Data*, *9*, 927–953. https://doi.org/10.5194/essd-9-927-2017

Klein Goldewijk, K., Beusen, A., van Drecht, G., & de Vos, M. (2011). The HYDE 3.1 spatially explicit database of human-induced global land-use change over the past 12,000 years. *Global Ecology and Biogeography*, *20*, 73–86. https://doi.org/10.1111/j.1466-8238.2010.00587.x

Kondo, M., Ichii, K., Patra, P. K., Canadell, J. G., Poulter, B., Sitch, S., et al. (2018). Land use change and El Niño-Southern Oscillation drive decadal carbon balance shifts in Southeast Asia. *Nature Communications*, *9*, 1154. https://doi.org/10.1038/s41467-018-03374-x

Kondo, M., Ichii, K., Patra, P. K., Poulter, B., Calle, L., Koven, C., et al. (2018). Plant regrowth as a driver of recent enhancement of terrestrial CO_2 uptake. *Geophysical Research Letters*, *45*(10), 4820–4830. https://doi.org/10.1029/2018gl077633

Kondo, M., Patra, P. K., Sitch, S., Friedlingstein, P., Poulter, B., Chevallier, F., et al. (2020). State of the science in reconciling top-down and bottom-up approaches for terrestrial CO_2 budget. *Global Change Biology*, *20*, 1068–1084. https://doi.org/10.1111/gcb.14917

Lawrence, D. M., Hurtt, G. C., Arneth, A., Brovkin, V., Calvin, K. V., Jones, A. D., et al. (2016). The Land Use Model Intercomparison Project (LUMIP) contribution to CMIP6: Rationale and experimental design. *Geoscientific Model Development*, *9*, 2973–2998. https://doi.org/10.5194/gmd-9-2973-2016

Le Quéré, C., Andres, R. J., Boden, T., Conway, T., Houghton, R. A., House, J. I., & Zeng, N. (2013). The global carbon budget 1959–2011. *Earth System Scientific Data*, *5*, 165–185.

Le Quéré, C., Andrew, R. M., Canadell, J. G., Sitch, S., Korsbakken, J. I., Peters, G. P., & Zaehle, S. (2016). Global carbon budget 2016. *Earth System Scientific Data*, *8*, 605–649.

Le Quéré, C., Andrew, R. M., Friedlingstein, P., Sitch, S., Hauck, J., Pongratz, J., et al. (2018). Global carbon budget 2018. *Earth System Scientific Data*, *10*(4), 2141–2194.

Le Quéré, C., Andrew, R. M., Friedlingstein, P., Sitch, S., Pongratz, J., Manning, A. C., et al. (2018). Global carbon budget 2017. *Earth System Scientific Data*, *10*, 405–448.

Le Quéré, C., Moriarty, R., Andrew, R. M., Canadell, J. G., Sitch, S., Korsbakken, J. I., & Zeng, N. (2015). Global carbon budget 2015. *Earth System Scientific Data*, *7*, 349–396.

Le Quéré, C., Moriarty, R., Andrew, R. M., Peters, G. P., Ciais, P., Friedlingstein, P., & Zeng, N. (2015). Global carbon budget 2014. *Earth System Scientific Data*, *7*, 47–85.

Le Quéré, C., Peters, G. P., Andres, R. J., Andrew, R. M., Boden, T. A., Ciais, P., & Zaehle, S. (2014). Global carbon budget 2013. *Earth System Scientific Data*, *6*, 235–263.

Lewis, S. L., Lopez-Gonzalez, G., Sonké, B., Affum-Baffoe, K., Baker, T. R., Ojo, L. O., et al. (2009). Increasing carbon storage in intact African tropical forests. *Nature*, *457*, 1003–1006. https://doi.org/10.1038/nature07771

Li, F., Bond-Lamberty, B., & Levis, S. (2014). Quantifying the role of fire in the earth system—Part 2: Impact on the net carbon balance of global terrestrial ecosystems for the 20th century. *Biogesciences*, *11*, 1345–1360. https://doi.org/10.5194/bg-11-1345-2014

Li, F., Levis, S., & Ward, D. S. (2013). Quantifying the role of fire in the earth system—Part 1: Improved global fire modeling in the community earth system model CESM1. *Biogesciences*, *10*, 2293–2314. https://doi.org/10.5194/bg-10-2293-2013

Maki, T., Ikegami, M., Fujita, T., Hirahara, T., Yamada, K., Mori, K., et al. (2010). New technique to analyse global distributions of CO_2 concentrations and fluxes from non-processed observational data. *Tellus Series B Chemical and Physical Meteorology*, *62*(5), 797–809. https://doi.org/10.1111/j.1600-0889.2010.00488.x

Mayaux, P., Holmgren, P., Achard, F., Eva, H., Stibig, H.-J. S., & Branthomme, A. (2005). Tropical forest cover change in the 1990s and options for future monitoring. *Philosophical Transactions of the Royal Society of London, Series B*, *360*, 373–384. https://doi.org/10.1098/rstb.2004.1590

Meijide, A., Röll, A., Fan, Y., Herbst, M., Niu, F., Tiedemann, F., et al. (2017). Controls of water and energy fluxes in oil palm plantations: Environmental variables and oil palm age. *Agricultural and Forest Meteorology*, *239*, 71–85. https://doi.org/10.1016/j.agrformet.2017.02.034

Mitchard, E. T. A. (2018). The tropical forest carbon cycle and climate change. *Nature*, *559*, 527–534. https://doi.org/10.1038/s41586-018-0300-2

Murdiyarso, D., Hergoualc'h, K., & Verchot, L. V. (2010). Opportunities for reducing greenhouse gas emissions in tropical peatlands. *Proceedings of the National Academy of Sciences of the United States of America*, *107*, 19655–19660. https://doi.org/10.1073/pnas.0911966107

Niwa, Y., Machida, T., Sawa, Y., Matsueda, H., Schuck, T. J., Brenninkmeijer, C. A. M., et al. (2012). Imposing strong constraints on tropical terrestrial CO_2 fluxes using passenger aircraft based measurements. *Journal of Geophysical Research*, *117*, D11303. https://doi.org/10.1029/2012jd017474

Page, S. E., Siegert, F., Rieley, J. O., Boehm, H.-D. V., Jaya, A., & Limin, S. (2002). The amount of carbon released from peat and forest fires in Indonesia during 1997. *Nature*, *420*, 61–65. https://doi.org/10.1038/nature01131

Patra, P. K., Ishizawa, M., Maksyutov, S., Nakazawa, T., & Inoue, G. (2005). Role of biomass burning and climate anomalies for land-atmosphere carbon fluxes based on inverse modeling of atmospheric CO_2. *Global Biogeochemical Cycles*, *19*, GB3005. https://doi.org/10.1029/2004gb002258

Patra, P. K., Maksyutov, S., Ishizawa, M., Nakazawa, T., Takahashi, T., & Ukita, J. (2005). Interannual and decadal changes in the sea-air CO_2 flux from atmospheric CO_2 inverse modelling. *Global Biogeochemical Cycles*, *19*, GB4013. https://doi.org/10.1029/2004gb002257

Pugh, T. A. M., Lindeskog, M., Smith, B., Poulter, B., Arneth, A., Haverd, V., & Calle, L. (2019). Role of forest regrowth in global carbon sink dynamics. *Proceedings of the National Academy of Sciences of the United States of America*, *116*(10), 4382–4387. https://doi.org/10.1073/pnas.1810512116

Qie, L., Lewis, S. L., Sullivan, M. J. P., Lopez-Gonzalez, G., Pickavance, G. C., Sunderland, T., et al. (2017). Long-term carbon sink in Borneo's forests halted by drought and vulnerable to edge effects. *Nature Communications*, *8*, 1966. https://doi.org/10.1038/s41467-017-01997-0

Saeki, T., & Patra, P. K. (2017). Implications of overestimated anthropogenic CO_2 emissions on East Asian and global land CO_2 flux inversion. *Geoscience Letters*, *4*(1), 9. https://doi.org/10.1186/s40562-017-0074-7

Schimel, D., Stephens, B. B., & Fisher, J. B. (2015). Effect of increasing CO_2 on the terrestrial carbon cycle. *Proceedings of the National Academy of Sciences of the United States of America*, *112*, 436–441. https://doi.org/10.1073/pnas.1407302112

Siegert, F., Ruecker, G., Hinrichs, A., & Hoffmann, A. A. (2001). Increased damage from fires in logged forests during droughts caused by El Nino. *Nature*, *414*, 437–440. https://doi.org/10.1038/35106547

Sitch, S., Friedlingstein, P., Gruber, N., Jones, S. D., Murray-Tortarolo, G., Ahlström, A., et al. (2015). Recent trends and drivers of regional sources and sinks of carbon dioxide. *Biogesciences*, *12*(3), 653–679. https://doi.org/10.5194/bg-12-653-2015

Stephens, B. B., Gurney, K. R., Tans, P. P., Sweeney, C., Peters, W., Bruhwiler, L., et al. (2007). Weak northern and strong tropical land carbon uptake from vertical profiles of atmospheric CO_2. *Science*, *316*(5832), 1732–1735. https://doi.org/10.1126/science.1137004

Stibig, H.-J., Achard, F., Carboni, S., Raši, R., & Miettinen, J. (2014). Change in tropical forest cover of Southeast Asia from 1990 to 2010. *Biogesciences*, *11*, 247–258. https://doi.org/10.5194/bg-11-247-2014

Thirumalai, K., DiNezio, P. N., Okumura, Y., & Deser, C. (2017). Extreme temperatures in Southeast Asia caused by El Niño and worsened by global warming. *Nature Communications*, *8*, 15531. https://doi.org/10.1038/ncomms15531

Uryu, Y. (2008). *Deforestation, forest degradation, biodiversity loss and CO_2 emissions in Riau, Sumatra, Indonesia*. WWF Indonesia technical report

Zeng, Z., Estes, L., Ziegler, A. D., Chen, A., Searchinger, T., Hua, F., et al. (2018). Highland cropland expansion and forest loss in Southeast Asia in the twenty-first century. *Nature Geoscience*, *11*, 556–562. https://doi.org/10.1038/s41561-018-0166-9

Ziegler, A. D., Phelps, J., Yuen, J. Q., Webb, E. L., Lawrence, D., Fox, J. M., et al. (2012). Carbon outcomes of major land-cover transitions in SE Asia: Great uncertainties and REDD+ policy implications. *Global Change Biology*, *18*, 3087–3099. https://doi.org/10.1111/j.1365-2486.2012.02747.x